Transactions of the Korean Society of Mechanical Engineers Vol. 4, No. 3, pp. 87~95 1980

<Original>

Analyses of Solidification Dynamics of Flowing Liquid in a Vertical Channel from a Reservoir

Moon-Hyun Chun*

(Received April 7, 1980)

저장조로부터 수직관 속을 흐르는 유체의 응고에 관한 해석

전 문 헌

초 록

일정한 압력으로 유지한 수직관속을 흐르는 유체의 응고에 관한 현상을 이론적으로 규명하고, 이미 얻은 실험 결과와 비교함으로서 그 정확성을 검토하였다. 관속을 흐르는 유체가 얼어서 완전히 관을 막을 때까지 요하는 시간을 산출하는 공식을 유도 하였으며 ' 관이 완전히 막힐 때까지 흘러내리는 유체의 양을 추정하는 방법도 제시하였다.

본 연구에서 제시한 공식의 적용 가능범위도 아울러 검토 하였다.

Nomenclature

A^* =dimensionless number, defined by Eq. (17)
B_i^* =effective Biot number, defined by Eq. (18)
C_p =specific heat, J/kgk
D_i =tube inside diameter, m
$F_i(R)$ =quantities defined by Eqs. (12-14), where i=1, 2, 3
g =acceleration due to gravity
h_{sf} =heat of fusion, J/kg
H_i =initial molten fluid head in the reservoir, m
K_1 =contraction loss coefficient
L =total length of the tube, m
$M(t)$ =transient mass displacement, kg
M_T =total mass displaced, kg
$\dot{M}_c$ =coolant water flow rate, kg/s
Δp =driving pressure behind the fluid, N/m²
r =radial coordinate, m
R =radius of liquid-solid interface, m
R_0 =intial channel radius, m
t =time, s
T =absolute temperature, K
T_c =coolant temperature, K
T_f =fusion temperature, K
T_∞ =sink temperure, K
Δt =freezing time and/or time required for complete channel plugging (with subscript p), s
v =fluid velocity, m/s
z =axial coordinate, m
α =exterior (with subscript e) and/or interior (with subscript i) heat transfer coefficient, W/m²K
α_{ov} =overall heat transfer coefficient W/m²k
δ_R =solidified shell, m
λ =thermal conductivity, W/mK
ρ =density, kg/m³
μ =viscosity, kg/m-s

Subscripts

l =liquid phase
s =solid phase
W =condition at the wall
1 =condition at the inlet of the channel
2 =condition at the exit of the channel

Superscripts

$*$ =dimensionless quantity

* 정 회원, 한국 과학원 핵 공학과

1. Introduction

The phenomenon of heat transfer and solidification of a flowing hot fluid is of interest in various applications, e.g., an immediate application fo this Phenomenon is to assess the dynamics of molten fuel relocation following a hypothetical core disruptive accident in a Liquid Metal Fast Breeder Reactor.

Solidification dynamics of flowing fluid through a vertical cooled channel with constant pressure end conditions have been studied using paraffin wax and Wood's metal as molten material in an earlier work (1). The purpose of this work is to present a simplified analytical model of the solidification process and examine the validity of this model by comparing with the experimental results obtained previously (1).

Nearly all the earlier works reviewed here except the existing model(2) have one of the following limitations or inherent drawbacks in their applicability, especially as relates to the molten fuel relocation phenomenon in a nuclear reactor: (a) the analyses are limited to the case of the solidification adjacent to a cooled flat surface (3-7), (b) analyses of freezing have been performed either for laminar flow conditions inside horizontal piping (8) or for the stationary fluid inside a cooled section of a closed channel (9), (c) none of the cited references explicitly analyzed the plugging times (i.e., the time required after freezing starts to completely block the tube so that no further flow can take place) and/or the transient mass displacement of the flowing and freezing fluids.

In summary, the previously reported analytical and experimental works (3-9), except the Ref. (2), do not enable one to estimate both the channel plugging time and the rate of fluid flow through a vertical cold channel from a reservoir where the liquid is subjected to the constant pressure.

The model developed here is based mainly on the experimental observations(1, 10) and on the existing computational model for freezing process (2). That is, the existing model (2) has been modified by introducing additional simplifying assumptions based on the experimental observations(1, 10) to improve its applicability and to allow one to predict the main variables of solidification dynamics. These include the complete channel plugging time and the transient mass displacement as a function of flowing time.

2. Analysis

2.1 Physical Model and Assumptions

A molten fluid at a fixed bulk temperature T_1 above its solidification temperature T_f suddenly begins to flow into a cylindrical channel, the walls of which are kept at a uniform temperature T_w below the freezing temperature of the flowing hot fluid by the countercurrent coolant flowing over the outer surface of the channel as shown in Fig. 1. The flowing molten fluid begins freezing at the inner surface of the tube and forms a solid shell of thickness δ_R which varies with both time and axial position along the tube. Solidification takes place as a result of continuous heat transfer from the flowing hot fluid to the colder solidified shell by convection. The heat convected from the flowing liquid is, in turn, removed by con-

duction through the solidified shell and tube wall which is cooled by convection of the coolant. Thus, solidification front moves radially into the liquid region at a rate determined by the convective heat flux from the flowing liquid to the phase interface and the rate at which the heat of solidification can be conducted away from the phase boundary to the solidifed shell and the tube wall (1).

In an annular co-axial counterflow heat exchanger system, the rate of solidification is the largest at the exit since both temperatures of the molten fluid and the coolant are the lowest. For the present system (Fig. 1), therefore, both the channel plugging time due to solidification and the transient mass displacement are primarily determined by the solidification rate at the channel exit. To take this fact properly into account, the following simplifying assumptions are made in addition to the assumptions introduced in the existing model (1):

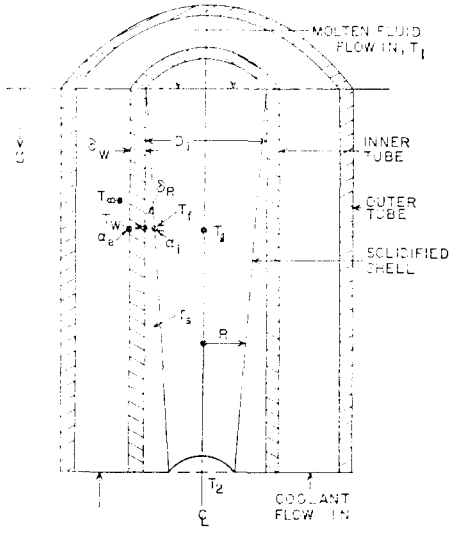

Fig. 1. Physical model of countercurrent flow test section.

a. The variation of the thickness of the solidified layer δ_R with both time and position along the tube axis is sufficiently small and a quasi-steady state can be assumed for radial heat conduction in the frozen layer.

b. The liquid flow characteristics inside the tube can be represented by a slug-flow velocity profile. For given initial and boundary conditions, the liquid exit velocity V_2 is a known quantity from existing correlations (e. g., modified Bernoulli equation which includes the appropriate friction terms) and remains constant with time (this assumption of constant velocity V_2 is removed only for computations of transient mass displacement). It has been observed numerically that results are insensitive to this assumption.

c. Axial heat conduction in the flowing liquid and in the solidified shell are negligible. The bulk liquid temperature at the tube exit T_2 remains constant with time.

d. The covective heat transfer coefficient between the flowing liquid and phase boundary α_i remains constant both with time and axial position along the tube. The existing heat transfer correlations developed for uniform wall temperature is applicable for the freezing process.

e. Both the exterior heat transfer coefficient α_e (which removes the radial heat flow the solidified shell and tube wall to the countercurrent coolant) and the heat sink temperature T_∞ remains constant with time and axial position along the tube.

f. A constant liquid head H_i is maintained in the reservoir above the inlet of the vertical channel and the pressure drop across the channel remains constant.

g. Physical properties for each phase are considered constant for given initial conditions.

The validity of the above simplifying assumptions may qualitatively be demonstrated by the general agreement between

the theory based on the above assumptions and the previous experimental results (10) of both paraffin wax and Wood's metal. It may be noted here that these two fluids were chosen based on their respective Prandtl numbers (about 40 and 0.018 for paraffin wax and Wood's metal, respectively, within the ranges of experimental conditions) (1, 10).

2.2 Theory and Correlations

For liquid phase, the heat transfer and the flow characteristics inside the tube are described according to the assumptions of b, c, d. The governing equation for the axial temperature distribution of the liquid phase is then found from an energy balance on a slug of fluid flowing in the channel (1);

$$\frac{dT}{dz}+\frac{2\alpha_i T}{\rho_l C_p V_2 R}=\frac{2\alpha_i T_f}{\rho_l C_p V_2 R} \tag{1}$$

for $0\le r\le R$, $z\ge 0$ and $t>0$. Appropriate boundary conditions are

$$T(r, o, t)=T_1 \quad t>0 \tag{2}$$

$$T(r, L, t)=T_2 \quad t>0 \tag{3}$$

From the assumptions of a and c, the governing equation for the solid phase is expressed as

$$\frac{d}{dr}\left(r\frac{dT_s}{dr}\right)=0 \qquad \text{for } R\le r\le R. \tag{4}$$

$$T_s(R, z, t)=T_f \tag{5}$$

$$-\lambda_s\left(\frac{\partial T_s}{\partial r}\right)_{R0}=\alpha_{ov}(T_w-T_\infty) \tag{6}$$

$$T_s(R_o, x, t)=T_w \tag{7}$$

Equations (1) and (4) are coupled by the interface energy balance equation. For the channel exit region, in particular, the energy balance may be written as

$$-\lambda_s\left(\frac{\partial T_s}{\partial r}\right)_R=\alpha_i(T_2-T_f)+\rho_l h_{sf}\left(-\frac{dR}{dt}\right) \tag{8}$$

The bulk fluid exit temperature T_2 is obtained by first applying the boundary conditions (2) and (3) in the solution of Eq. (1), and approximating the result according to the assumption c;

$$T_2=(T_1-T_f)\exp\left(-\frac{2\alpha_i L}{\rho_l C_p V_2 R_o}\right)+T_f \tag{9}$$

On the other hand, the temperature profile within the solidified region at the exit of the channel ($z=L$) is obtained from Eq. (4) along with the boundary conditions of (5) and (6) as

$$T_s(r,\ L)=T_f-\frac{R_o\alpha_{ov}}{\lambda_s}(T_w-T_\infty)\ln\frac{r}{R} \tag{10}$$

for $R\le r\le R_o$. Similarly, inner tube wall temperature at the exit is obtained as

$$T_w(R_o,\ L)=\frac{F_1(R)+F_2(R)}{F_3(R)} \tag{11}$$

where

$$F_1(R)=\lambda_s T_f \tag{12}$$

$$F_2(R)=R_o\alpha_{ov}T_\infty\ln\frac{R_o}{R} \tag{13}$$

$$F_3(R)=\lambda_s+R_o\alpha_{ov}\ln\frac{R_o}{R} \tag{14}$$

Solidification rate at the exit is then found by combining Eqs. (10) and (11), and substituting the results and Eq. (9) into the interface energy balance Eq. (8) as

$$-\frac{dR}{dt}=\frac{\dfrac{R_o\alpha_{ov}\lambda_s}{R}(T_f-T_\infty)-\alpha_i(T_2-T_f)\left(\lambda_s+R_o\alpha_{ov}\ln\dfrac{R}{R_o}\right)}{\rho_l h_{sf}\left(\lambda_s+R_o\alpha_{ov}\ln\dfrac{R_o}{R}\right)} \tag{15}$$

By introducing $R^*=\frac{R}{R_0}$ in Eq. (15) and rearranging the results

$$-\frac{dR^*}{dt^*}=\frac{1-A^*(1-B_i^*\ln R^*)R^*}{(1-B_i^*\ln R^*)R^*} \tag{16}$$

where

$$A^*=\frac{\alpha_i(T_2-T_f)}{\alpha_{ov}(T_f-T_\infty)} \tag{17}$$

$$B_i^* = \frac{R_o \alpha_{av}}{\lambda_s} \tag{18}$$

$$t^* = \frac{t\alpha_{av}(T_f - T_\infty)}{\rho_l h_{sf} R_o} \tag{19}$$

The time required to solidify from an initial radius R_0(i.e., $R^*=1$) to a new radius R^* is obtained by integration of Eq. (16) as

$$\Delta t^* = \int_{R^*}^{1} \frac{(1 - B_i^* \ln R^*) R^* dR^*}{1 - A^*(1 - B_i^* \ln R^*) R^*} \tag{20}$$

The dimensionless channel plugging time Δt_p^*, in particular, can be found from Eq. (20) simply replacing the lower limit R^* with zero. This integral can easily be performed by the Sim pson's role.

For the special case when the inlet temperature of the molten fluind T_1 is at its solidification temperature $T_2=T_f$ (note that $A^*=0$ when $T_2=T_f$), Eq. (20) reduces to the following simple formula;

$$(\Delta t_p^*)_{T_1=T_f} = 1/4(2+B_i^*) \tag{21}$$

Transient mass displacement may be computed from the modified Bernoulli equation using appropriate values of laminar or turbulent friction factors and the instantaneous channel flow area.

That is, fluid velocity for laminar flow regime is found from the solution of the following equation:

$$V_2^2(1+K_1) + V_2\left(\frac{16\mu L}{\rho_l R_2^2}\right) = \frac{2\Delta P}{\rho_l} + 2g(H+L) \tag{22}$$

Fluid velocity for turbulent flow regime, on the other hand, is estimated from the following relation:

$$V_2^2(1+K_1) + V_2^{1.8}\left[\frac{0.08L}{R_2^{1.2}}\left(\frac{\mu}{\rho_l}\right)^{0.2}\right] = \frac{2\Delta P}{\rho_l} + 2g(H+L) \tag{23}$$

In the above equation, the entrance loss coefficient K_1 is determined experimentally. Once the channel radius R_2 and the fluid velocity V_2 are determined, the transient mass displacement is found from

$$M(t) = \rho_l V_2 \pi R_2^2 \Delta t \tag{24}$$

Where Δt is the time interval for the radius R_2 to change from one radius to another due to solidification of the flowing fluid.

The interfacial heat transfer coefficient α_i for laminar flow (e. g., paraffin wax test results of Refs. 1 and 10) and turbulent flow for liquid metal (Wood's metal test results of Refs. 1 and 10 were applicable) are obtained from Sieder and Tate(11) and Seban and Shimazaki(12) correlations, respectively, whereas the coolant flow heat transfer is estimated from the Dittus-Boelter equation.

3. Comparison with Experimental Results and Discussions

Experimental results of transient mass displacement and channel plugging time(or time at which essentially all the available mass has been displaced) were obtained both for paraffin wax and Wood's metal in an earlier work (1, 10). These are summarized and compared with predictions of theory and presented in Table 1(1).

3.1 Total Mass Displaced and Plugging Time

Agreement between mean values of experiment and theory for the total mass displacement is within 9~31% aud 17~51% for paraffin wax(up to T_1=348k) and for Wood's metal(up to T_1=378k), respectively. On the other hand, the agreement for the plugging times is within 6~10% for paraffin wax up to T_1=348k(with one exception at T_1=348k; At this temperature an extremely large deviation occurred. The deviation may be partly attributable to some uncertainties in

Table 1. Comparison of experimental results with predictions of theory

Test Conditions			Experimental Results (1, 10)					Predictions of Theory	
Test Fluid	T_1 (K)	ΔP (N/m²)	No. of Runs Repeated	Mean Value of M_T(kg)	Standard Deviation of M_T(kg)	Mean Value of Δt_P (sec)	Standard Deviation of Δt_P (sec)	M_T (kg)	Δt_P (sec)
Paraffin Wax	328	0	3	0.034	0.0037	21.6	1.4	0.037	23.0
	338	0	4	0.090	0.0156	34.4	2.7	0.066	37.9
	348	0	3	0.112	0.0025	43.3	0.7	0.147	141.7
	358	0	3	0.176	0.0407	65.5	13.7	—	**112.0
	368	0	3	0.346	0.1472	123.6	39.3	—	**84.8
Wood's Metal	348	6894.7	4	8.483	1.642	12.6	1.8	4.150	6.8
	363	6894.7	5	8.412	1.296	13.5	0.8	5.768	9.8
	378	6894.7	5	12.054	2.410	17.7	1.8	10.014	18.5
	398	6894.7	6	*19.431	0.588	*18.8	4.2	*19.488	*15.6
	408	6894.7	5	*19.490	0.338	*15.0	2.3	*20.163	*13.2

T_c=298 K, H_i=0.136m, $\dot{M}_c$=0.32kg/s for paraffin wax and 0.22kg/s for Wood's metal.

* : Time at which essentially all the available mass has been displaced and/or the corresponding displaced mass.

** : Time at which an equilibrium condition occurs.

the physical properties and heat transfer coefficients used. However, the main reason seems to be the effect of the sensitivity of the heat balance on the plugging time at higher superheat levels). For Wood's metal plugging time the agreement between experiment aud theory is about 5~46% up to T_1=378k.

Predictions of theory for paraffin wax at higher superheat levels (i. e., T_1=358k and T_1=368k) show that equilibrium conditions occur(such that no more solidification takes place) before complete channel plugging. Fxperimental results for these cases show also an extremely longer period of time was required to plug. For Wood's metal test(1, 10) at higher superheat (T_1=398k and T_1=408k) showed that all the available mass was displaced prior to complete plugging.

3.2 Transient Mass Displacement

Transient mass displacement versus ltime are shown in Figs. 2-5 along with the theoretical curves. Experimental curves in these figures are the representative curves for each inlet temperature level. Agreement is generally good except at T_1=348k (superheat of 2k) for Wood's metal. The main reason for the deviation between theory and expe-

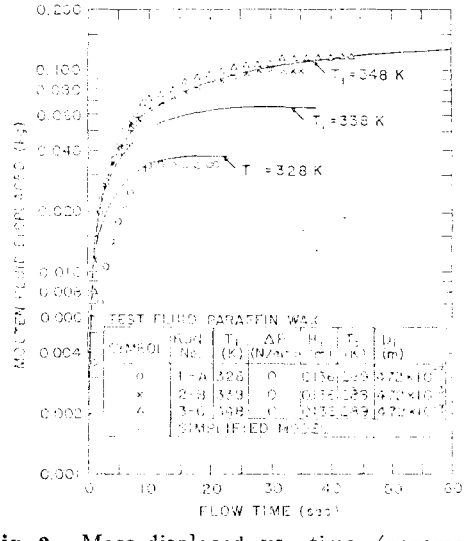

Fig. 2. Mass displaced vs. time (parameter: inlet temperature T_1)

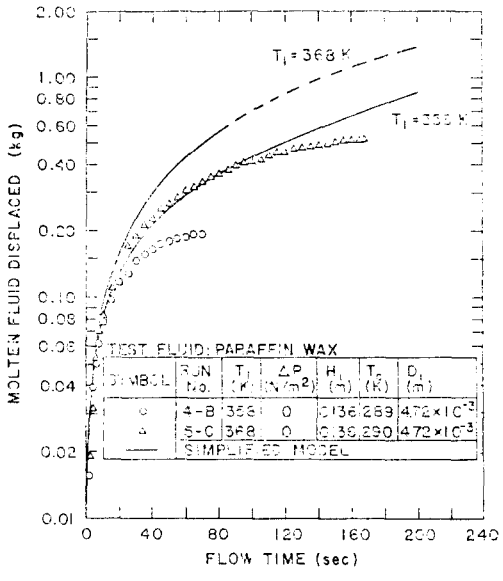

Fig. 3. Mass displaced vs. time (parameter: inlet temperature T_1)

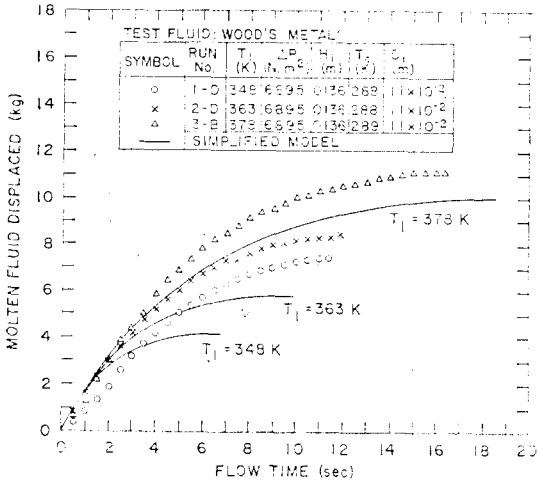

Fig. 4. Mass displaced vs. time (parameter: inlet temperature T_1)

riment for this case may be due to the inherent characteristics of the molten Wood's metal that exist at a temperature close to the solidfication point; the molten Wood's metal flowing through the inner tube of the counterflow heat exchanger system (1, 10)

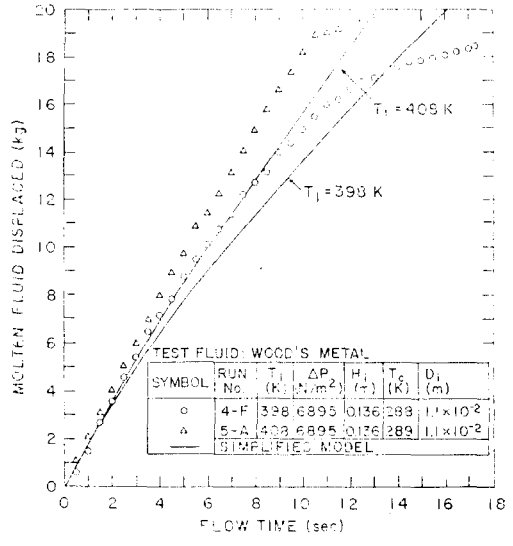

Fig. 5. Mass displaced vs. time (parameter: inlet temperature T_1)

tends to approach toward an annular flow (i.e., a non-slug flow) where the contact area between the flowing fluid and the solidified layer decreases, thereby reducing the solidification rate, whereas a slug flow is assumed to exist for all cases in the present model.

Thermophsical properties of the paraffin wax and the Wood's metal used in the present work are summarized in Table 2.

Table 2. Properties of paraffin wax and wood's metal (1, 10)

	Paraffin Wax		Wood's Metal
	Solid (289-325k)	Liquid (325-373k)	(289-418k)
Melting Point (K)	325	···	346
Heat of Fusion (KJ/kg)	175.8	···	46.5
Density (kg/m³)	910-810	797-788	9,200
Thermal Conductivity (W/mK)	0.28	0.20	13.4
Specific Heat (J/kgk)	2093-2302	2428-2511	150-178
Viscosity (kg/ms)	0.06	0.036-0.031	0.016
Prandtl mumber		43.5-38.8	0.018

3.3 Applicable Range of Theory

To examine the applicable range of the theory (Eq, 16 or Eq. 20) a dimensionless plugging time (Δt_p^*) is plotted against a dimensionless parameter A^* using B_i^* as a parameter and the results are shown in Fig. 6. From these results and all the comparisons of the experimental results and theory a conclusion may be made as follows:

(1) In general, the plugging time can be predicted from the present theery (Eq. 20) which agrees with the experimental results within $\pm$ 50% for up to $A^*=0.015$ and $A^*=.37$ when B_i^* is 133.9 and 5.4, respectively. It is interesting to note that the theory is applicable for up to $A^*\cdot B_i^*=2.0$.

(2) For mass displacement, the theory agrees with the experiment within $\pm$50% for up to $A^*\cdot B_i^*\simeq 5$.

Notice that B_i^* is an "effective Biot number", whereas A^* may be interpreted as the ratio between the "heat flow from the flowing fluid to the solidified shell" and the "heat flow from the solidified shell to the coolant" at steady state (evaluated at the channel exit). The product $A^*\cdot B_i^*$, on the other hand, may be described as the "condition of heat balance between the flowing fluid and the solidified shell at steady state and at the time of complete channel plugging."

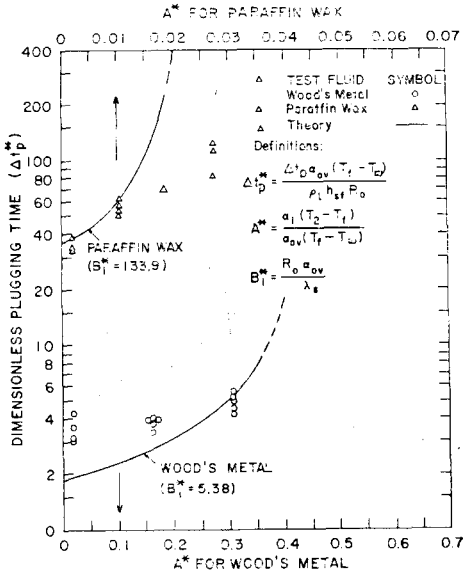

Fig. 6. Dimensionless plugging time (Δt_p^*) vs. a dimensionless parameter A^* (B_i^* as a parameter)

3.4 Parametric Effects

The results of the tests (1, 10) with paraffin wax and Wood's metal showed that the plugging time as well as the total mass displaced prior to plugging increased as the molten fluid inlet temperature level increased when other conditions were held constant. This result is in complete agreement with physical reasoning.

As may be observed from Eq. (21), when the inlet temperature of the molten fluid is at its solidification temperature, a unique parameter for the channel plugging time is the "effective Biot number B_i^*" and the channel plugging time is linearly proportional to B_i^*. Thus, from the definition of B_i^* (Eq. 18) and Eq. (21) it is clear that the channel plugging time increases as the initial radius R_o increases or the thermal conductivity (λ) of the fluid decreases, while the overall heat transfer coefficient (α_{ov}) is held constant. This is in complete agreement with the experimental results of both paraffin wax and Wood's metal; At close to the solidification point (superheat of about 2°C) the channel plugging times were 21 seconds and 12.6 seconds for the paraffin wax (whose thermal conductivity is 0.2-0.28

W/mK, and D_i and α_{ov} were 0.47cm and 15906.8 W/m^2-K, respectively) and the Wood's metal (whose thermal conductivity is 13.4 $W/m-K$ and D_i and α_{ov} were 1.1cm and 12976.6W/m^2-K), respectively.

When the inlet temperature of the molten fluid is above its solidification point the solidification rate for the present system (Fig. 1) can be represented by the two parameters (see Eq. 20), i.e., A^* and B_i^* (or their product $A^*\cdot B_i^*$).

4. Conclusions

A theoretical work on solidification dynamics of a flowing molten fluid through a vertical channel, the walls of which are cooled below the freezing temperature of the fluid from a constant pressure reservoir is presented and compared with the experimental results obtained previously (1, 10) to examine the validity of the model. An explicit theoretical model for the channel plugging time is presented along with simple methods that allow one to estimate the transient mass displacement as a function of flowing time. Comparison of the experimental results of both paraffin wax and Wood's metal with the theory shows that the present theory for plugging time is applicable for A^* less than 0.015 and 0.37 when B_i^* is about 134 and 5.4, respectively. It can be inferred from this conclusion that the present simplified model for the channel plugging time can be applied to estimate the downward relocation rates of the molten fuel following a hypothetical core disruptive accident in an LMFBR for wide range of conditions comparable to $A^*\cdot B_i^*$ less than 2.0 (1, 10).

References

1. Chun, M.H., Solidification Dynamics of Flowing Liquid in a Vertical channel from a Reservoir, BNL-NUREG-23149, Brookhaven National Laboratory, 1977.
2. Gasser, R .D., and Kazimi, M.S., Nuclear Technology, Vol. 33, p. 248-259, 1977.
3. Libby, P.A., and Chen, S., Int. J. Heat Mass Transfer, Vol. 8, p. 395-402, 1965.
4. Lapadula, C., and Mueler, W.K., Int. J. Heat Mass Transfer, Vol. 9, p. 702-704, 1966.
5. Beaubouef, R.T., and Chapman, A.J., Int. J. Heat Mass Transfer. Vol. 10, p. 1581-1587, 1967.
6. Savine, J.M., and Siegel, R., Int. J. Heat Mass Transfer, Vol. 12, p. 803-809, 1969.
7. Elmas, M., Int. J. Heat Mass Transfer, Vol. 13, p. 1060-1062, 1970.
8. Zerkle, R.D., and Sunderland, J.E., Transactions ASME J. Heat Transfer, Vol. 90, p. 183-190, 1968.
9. Hirschberg, H.G., Kaltetechnik, Vol. 14, p. 314-321, 1962.
10. Chun, M.H., Barry, J.J., Kazimi, M.S., Ginsberg, T., and Jones, O.C. Jr., Solidification Dynamics of Flowing Fluids, BNL-NUREG-24616, Brookhaven National Laboratory, 1977.
11. Sieder, E.N., and Tate, G.E., Ind. Eng. Chem., Vol. 28, p.1429-1435, 1936.
12. Seban, R.A., and Shimazaki, T., ASME paper 50-A-128, 1950.